Zoologischer Anzeiger 284 (2020) 78–87

Contents lists available at ScienceDirect

Zoologischer Anzeiger

journal homepage: www.elsevier.com/locate/jcz

Research paper

Increasing our knowledge on direct-developing frogs: The ontogeny of *Ischnocnema henselii* (Anura: Brachycephalidae)

Javier Goldberg [a, *], Pedro P.G. Taucce [b], Silvia Inés Quinzio [a], Célio F.B. Haddad [b], Florencia Vera Candioti [c]

[a] Instituto de Bio y Geociencias del NOA (IBIGEO-CONICET), CCT-Salta-Jujuy, Rosario de Lerma, Salta, Argentina
[b] Instituto de Biociências, UNESP - Universidade Estadual Paulista (UNESP), Câmpus Rio Claro, Departamento de Zoologia e Centro de Aquicultura (CAUNESP), Rio Claro, SP, Brazil
[c] Unidad Ejecutora Lillo CONICET–FML, San Miguel de Tucumán, Argentina

ARTICLE INFO

Article history:
Received 8 August 2019
Received in revised form
25 October 2019
Accepted 5 November 2019
Available online 14 November 2019

Corresponding Editor: Alexander Kupfer

Keywords:
Brachycephaloidea
Development
Embryo
Morphological characters
Thyroid

ABSTRACT

Due to the difficulty in finding newly fresh spawn in natural environments, few embryonic developmental studies have been carried out in anurans with direct development. Here we provide detailed data on the embryonic ontogeny of *Ischnocnema henselii*, and compare some morphological aspects related to its developmental mode within and outside of the brachycephaloid clade. Embryonic development in *I. henselii* is characterized by a unicuspid egg tooth (bicuspid in most other Brachycephaloidea), external gills present, open vent tube, and tail fins with dorsoventral orientation throughout the development. We also provide the first account of skin development in direct-developing frogs, revealing that the maturation of the integument has a typical dorsal to ventral sequence of changes as in most biphasic anurans. The early onset of thyroid development seems to be consistent with the hypothesis that the evolution of direct development in anuran amphibians involved precocious activation of the thyroid axis. A comparative analysis with the still few described embryonic ontogenies for direct-developing species reveals variation in the length of the embryonic period, rate of development, size at hatching and presence/absence of external morphological characters, which suggests heterochronic shifts in the rate of species-specific stage progression. All these details reinforce the idea of the high morphological variability among direct-developing frogs.

1. Introduction

The study of ontogenetic changes requires approximations that allow temporal ordering of phenotypic variation. In different groups, development tables have been proposed with a subdivision into discrete and ordered stages, each of which is 'an arbitrarily cut section through the time-axis of the life of an organism' (de Beer 1940). The temporal order (sequence) allows us to compare individuals in stages of ontogeny that we define as equivalent.

In anurans, two tables of embryonic and larval development are widely used: the table by Nieuwkoop and Faber (1967) for *Xenopus laevis* (Daudin, 1802) that describes 66 stages from fertilization to complete absence of tail, and Gosner table (Gosner 1960) that summarizes the embryonic and larval development of *Incilius valliceps* (Wiegmann, 1833) in 46 stages. These tables, especially the second one, have been used extensively to describe ontogenies of most other anuran taxa. Species-specific staging tables have been only constructed for 2% of extant species (Fabrezi et al. 2017), which represents an insignificant fraction of the anuran diversity. For direct-developing species this proportion is even lower, though efforts are growing to increase our knowledge.

Townsend and Stewart (1985) proposed a table of normal development for the brachycephaloid *Eleutherodactylus coqui* Thomas, 1966, and discussed some morphological and heterochronic variations reported in other *Eleutherodactylus* Duméril and Bibron, 1841 species and related genera (Sampson 1904; Noble 1925; Lynn 1942; Gitlin 1944; Lynn & Lutz 1946, 1947; Jameson 1950; Hughes 1959; Adamson et al. 1960; Valett & Jameson 1961). Further descriptions of direct-developing species in and out of Brachycephaloidea Günther 1858 have become available

* Corresponding author.
E-mail addresses: jgoldberg@conicet.gov.ar (J. Goldberg), pedrotaucce@gmail.com (P.P.G. Taucce), squinzio@conicet.gov.ar (S.I. Quinzio), haddad1000@gmail.com (C.F.B. Haddad), florivc@gmail.com (F. Vera Candioti).

https://doi.org/10.1016/j.jcz.2019.11.001
0044-5231/

since then (a recent compilation in Schweiger et al. 2017). A comparative analysis of these few species reveals that embryonic development in direct-developing species is not as conserved as once thought.

As currently defined, the large Neotropical clade Brachycephaloidea includes ca. 1150 species apparently all characterized by having direct development (Hedges et al. 2008; Heinicke et al. 2009; Pyron & Wiens 2011; Taboada et al. 2013; Padial et al. 2014). However, apart from *E. coqui*, studies describing embryonic development in the group exist for only a few species of *Adelophryne* Hoogmoed and Lescure, 1984 (de Lima et al., 2016), *Brachycephalus* Fitzinger, 1826 (Pombal, 1999), *Craugastor* Cope, 1862 (Valett & Jameson, 1961), *Eleutherodactylus* (Gitlin, 1944; Jameson, 1950), *Haddadus* Hedges, Duellman, and Heinicke, 2008 (Goldberg & Vera Candioti, 2015), *Ischnocnema* Reinhardt and Lütken, 1862 (Lynn & Lutz, 1946, 1947), *Oreobates* Jiménez de la Espada, 1872 (Goldberg et al., 2012), and *Pristimantis* Jiménez de la Espada, 1870 (Nokhbatolfoghahai et al., 2010). All of these descriptions show some differences with respect to the staging table by Townsend and Stewart (1985), and this highlights that more detailed characterizations are needed to address morphological diversity and evolution within the clade.

The genus *Ischnocnema* comprises 37 species of leaf-litter dwelling frogs, distributed in central and southern Brazil, adjacent northern Argentina, and possibly reaching into adjacent Paraguay (Taucce et al. 2018a; Frost 2019). Here we describe the embryonic development of *Ischnocnema henselii* (Peters, 1870), which occurs in subtropical Atlantic rainforest and parts of the Araucaria forest of southern and southeast (Serra do Mar) Brazil and Misiones, Argentina (Lucas et al. 2018; Frost 2019). Despite its wide distribution, and several studies analyzing the microhabitat use (Santos-Pereira et al. 2015), diet and feeding behavior (Dietl et al. 2009), conservation status (Vaira et al. 2012; Foerster & Conte 2018), and its taxonomy and systematic position (Taucce et al. 2018a, b), nothing is known about its early development. Thus, in this article we provide detailed data on the embryonic ontogeny of *I. henselii* and discuss some morphological aspects related to its developmental mode. We also provide the first account of skin development in direct-developing frogs and discuss its possible relationship with thyroid development. Increasing our knowledge of the embryonic development in direct-developing species adds new information to discuss the varied ontogenetic pathways involved in this developmental mode that, although widespread among anurans, has received comparatively little attention.

2. Materials and methods

A terrestrial clutch (33 viable eggs) was collected in December 2014, in Jaraguá do Sul (state of Santa Catarina, Brazil), and then incubated at room temperature (20–25 °C) in a plastic container with a lightly moistened, disaggregated *Sphagnum*. We preserved one egg in 99.5% ethanol at the moment of collection, and the rest of the sample was periodically fixed in 10% formalin, initially every 8 h and later every 24/48 h when morphological changes were evident. In order to identify the species, we extracted whole DNA from the ethanol-preserved egg following Lyra et al. (2017) and performed PCR amplifications of the mitochondrial 16S rRNA fragment limited by the primers 16SAR and 16SBR (Palumbi et al. 1991) following Taucce et al. (2018b). Purification also followed Lyra et al. (2017) and we sequenced the fragment with a BigDye Terminator Cycle Sequencing Kit (version 3.0, Applied Biosystems) in an ABI 3730 automated DNA sequencer (Applied Biosystems) at Macrogen Inc. (Seoul, South Korea). We then used the BLAST tool (Madden 2002) against GenBank sequences. Because GenBank is not a static database, and in order to make our results reproducible, we took GenBank sequences (Table S1) from both *Ischnocnema* species we found in the study area, *I. henselii* ($n = 57$ sequences) and *I.* cf. *manezinho* ($n = 1$ sequence) and constructed a matrix adding the egg sequence. We performed the alignment using MAFFT v7.130b (Katoh & Standley 2013) using the E-INS-i algorithm and computed genetic distances with packages APE 5.1 (Paradis et al. 2004) and SPIDER 1.4–2 (Brown et al. 2012) of the R platform version 3.3.3 (R Core Team 2017). Because we wanted to decrease the effect of the alignment, we ignored indels in a pairwise way (*pairwise.deletion*=T in the *dist.dna* function). We staged embryos following the table for *E. coqui* by Townsend and Stewart (1985) (TS from here) and differences were highlighted when relevant. At first mention of each stage, we state the estimated number of days post-fertilization as '(ca. d.p.f.)'. Morphological features, measurements, and photographs were obtained with a Leica M205 stereomicroscope. For histological cross-sections of the tail, skin, and thyroid glands, three embryos at TS6, TS13, and TS14 were dehydrated, embedded in paraffin, and sectioned at 6 μm. Sections were stained with hematoxylin and eosin following the protocol by Martoja and Martoja-Pierson (1970). We observed histological sections with a Nikon (Nikon Corp., Tokyo, Japan) E200 light microscope equipped with a digital camera. Finally, three further specimens (TS5, TS8, and TS14) were dehydrated using serial dilutions of ethanol and coated with gold to be examined with a Zeiss Supra 55VP scanning electron microscope. Voucher specimens are housed at the amphibian collection Célio F. B. Haddad, Departamento de Zoologia, Instituto de Biociências, Universidade Estadual Paulista, Campus de Rio Claro, São Paulo, Brazil, as a single lot numbered CFBH 39509.

3. Results

3.1. Species identification

The pairwise genetic distance between our egg sequence (GenBank accession number MN608783) and the sequences from *I. henselii* ranged from 0.0% (specimens from the municipalities of Anitápolis, Rancho Queimado, São Bonifácio, and Treviso, state of Santa Catarina, and São Francisco de Paula, state of Rio Grande do Sul) to 4.5% (specimen from the municipality of São Luíz do Paraitinga, state of São Paulo), whereas the distance between our sequence and that of *I.* cf. *manezinho* was 19.3%. The BLAST tool analysis resulted in the same closest sequences, with 99.77% of identity. It was not 100% because BLAST takes indels into account and our sequence have one deletion in comparison with the other sequences. *Ischnocnema* cf. *manezinho* did not appear in the 100 closest sequences list resulted from BLAST. This results leaves no doubt that our clutch belongs to *I. henselii*.

3.2. Size and time

The clutch of *I. henselii* was found in a region characterized by Montane Ombrophilous Dense Forests within the Brazilian Atlantic rainforest domain (IBGE 2012). Embryos were at TS4. Thus, based on the literature (Townsend & Stewart 1985; Lynn & Lutz 1946, 1947; Goldberg et al. 2012) we estimate eggs were laid two to three days before. Following this, we estimate that development from fertilization to hatching lasts about 28–30 days in this species. Egg size increases from TS4 (ca. 3 d.p.f.) with average diameter = 2.78 mm to TS14 (ca. 21 d.p.f.) = 5.21 mm. A hatched specimen has a snout-vent length equaling 6.71 mm, meaning that posthatching growth involves a fourfold length increase.

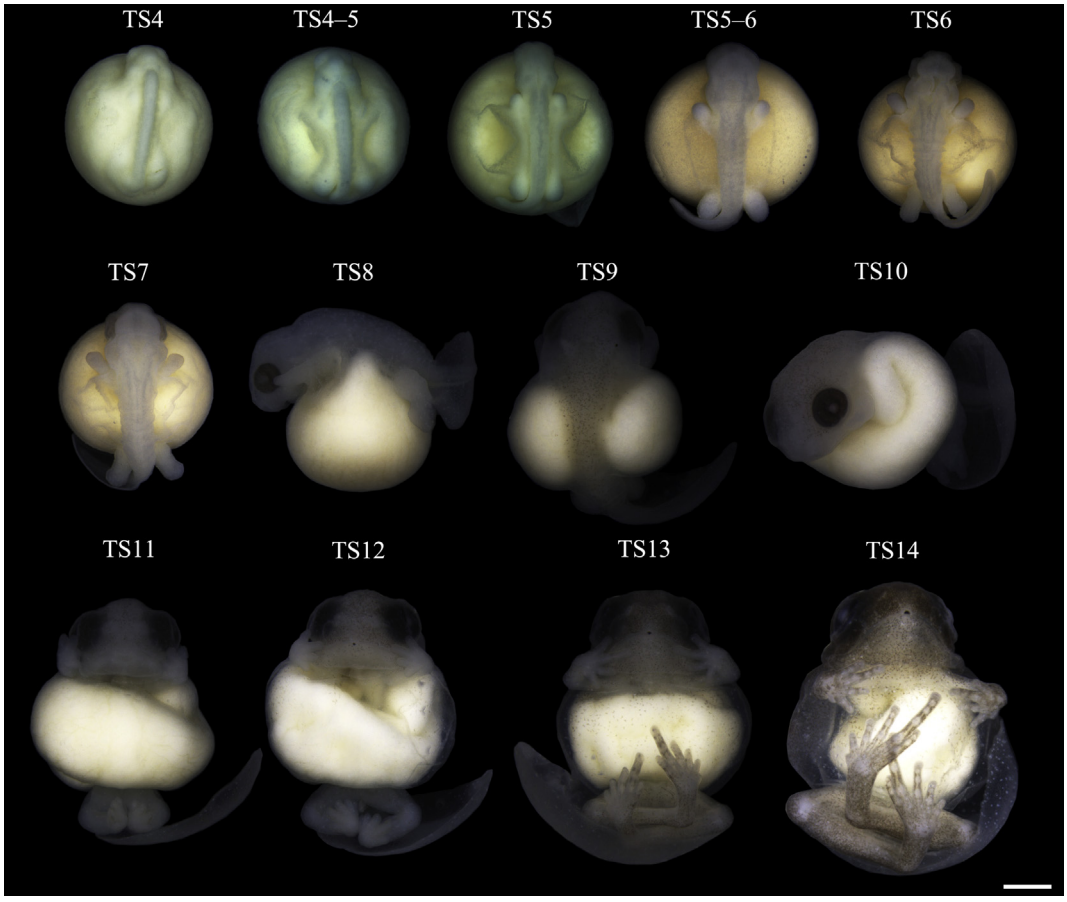

Fig. 1. External development in pre-hatching stages of *Ischnocnema henselii*. Jelly layers have been removed. Note the tadpole-like arrangement of the tail. Scale bar = 1 mm.

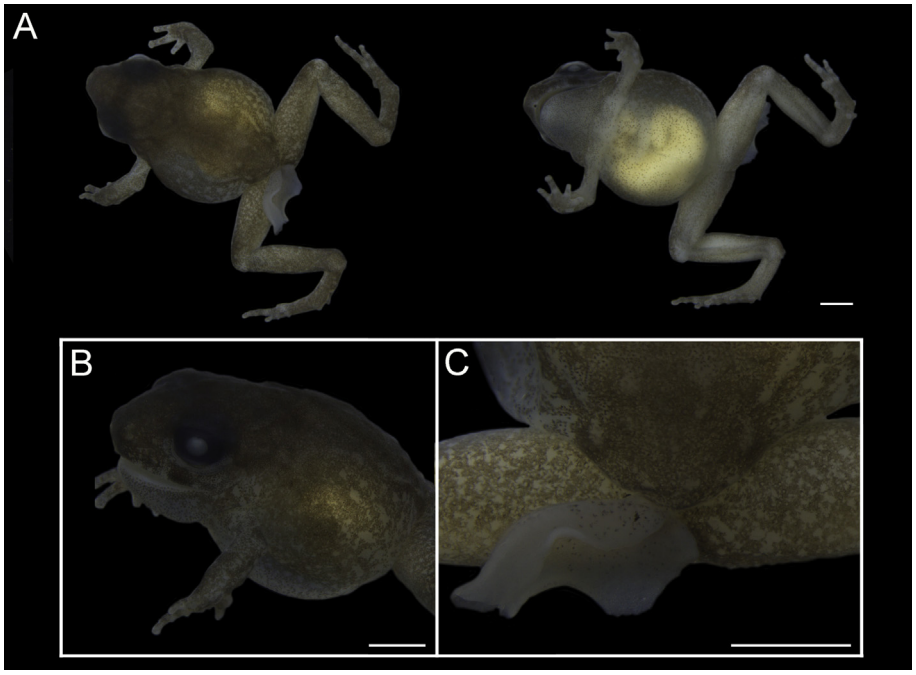

Fig. 2. Hatched specimen of *Ischnocnema henselii*. Dorsal and ventral views (A), and details of the body (B) and caudal region (C). Note the persisting yolk and the vestigial tail fins. Scale bars = 1 mm.

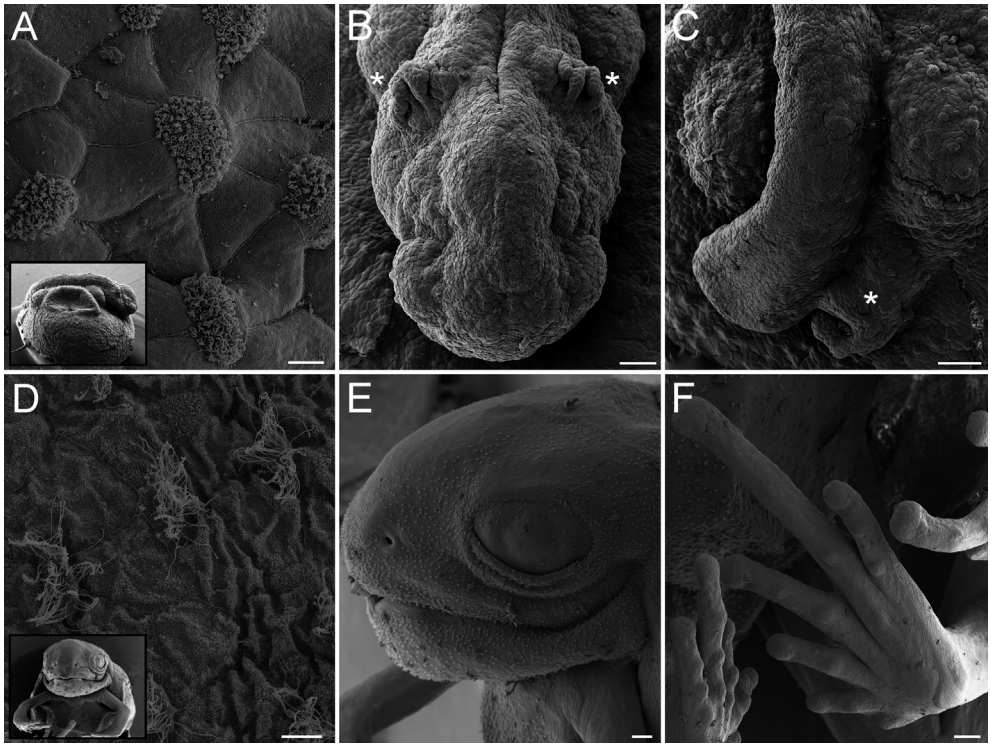

Fig. 3. Scanning electron micrographs of specimens of *Ischnocnema henselii* at TS5 (top) and TS14 (bottom); insets show specimens at low magnification. (A) Detail of ciliated cells from the dorsal body. (B) External gills at full development. (C) Ciliated hind limbs and vent tube differentiated. (D) Ciliated cells still present on most body surface. (E) Angle of the mouth post-orbital and rostral and dorsal region of the head lacking ciliation. (F) Subarticular tubercles differentiated on fore- and hind limbs. Scale bars = 100 μm excepting A and D = 10 μm.

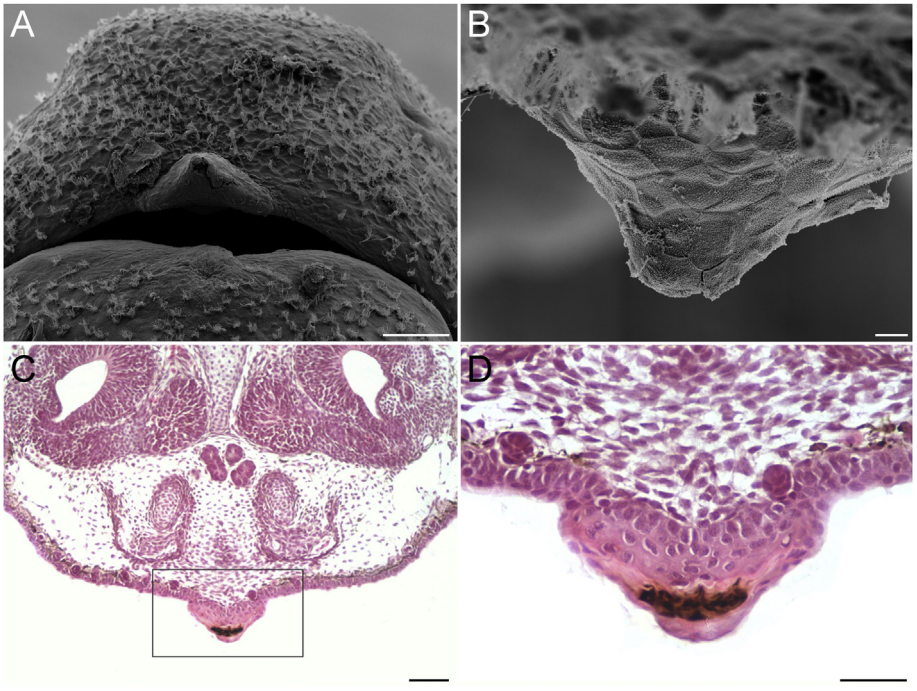

Fig. 4. Egg tooth of *Ischnocnema henselii* at TS14. Scanning electron micrographs showing the placement (A) and monocuspid morphology (B). Histomorphology of the upper jaw region (C) and detail of the thickened epidermis with accumulation of keratin evident. Scale bars = 100 μm (A, B, C) and 50 μm (D).

3.3. Cephalic region (Figs. 1–4)

By TS4 the head is differentiated from the rest of the body and the stomodeum can be recognized as a slight depression. The eyes appear as large anterior protuberances without pigmentation. A pair of gill buds is already present at the beginning of the stage, appearing as small protuberances posterior to the eyes, and reach their maximum development by the end of the stage. Next, eyes become more prominent but not yet pigmented. Gills are still evident at TS5 (ca. 4 d.p.f.; Fig. 3A and B) and regress soon after. By TS6 (ca. 7 d.p.f) the mouth changes from a terminal to a subterminal position. The eyes are now prominent, light gray and have distinct pupils. During TS8 (ca. 10 d.p.f.), the mouth opens and the lower and upper jaws are differentiated. Eyes become darker. By TS9 (ca. 12 d.p.f.), the mouth extends laterally at each corner to a point anterior to each eye. At TS10 (ca. 13 d.p.f.), the end of the lower jaw lagged far behind the upper jaw and the egg tooth appears as a small, non-keratinized, monocuspid structure. At the next stage, nostrils are evident. By TS13 (ca. 19 d.p.f.) the lacrimal groove extends from each nostril to the eyes and the canthus rostralis is evident. The lower eyelid is distinct. The angle of the mouth acquires its definitive arrangement, posterior to the eye, at TS14 (Fig. 3D and E). As development progresses, the egg tooth becomes larger and darkly keratinized (Fig. 4) and is present in the single hatched specimen (Fig. 2).

3.4. Limbs (Figs. 1–3)

Fore- and hind limbs appear at middle TS4 as rounded buds joined to the trunk. Limbs project at an angle of 45° as they grow, and by TS5 a dermal fold continuous with the epidermis of the body covers the base of each forelimb. As this stage progresses, limb buds become more oblong. Hind limbs are slightly advanced in development and larger than forelimbs. By TS6 both anterior and posterior constrictions that delimit the hind limb autopodium appear. In the next stage, both limbs show paddle-shape autopodia morphology. By TS8 the elongation of digit IV (primary axis) is noticeable. Dermal folds acquire their maximal coverage and enclose the proximal part of each forelimb. From the next stage on, all fingers and toes begin their differentiation and by TS11 (ca. 14 d.p.f) they are all individualized; hind limbs arrange with heels held together. Later, by TS13, hind limbs cross each other, fingers and toes lengthen, and inner metatarsal and metacarpal tubercles differentiate. Subarticular tubercles are distinct in hands and feet of TS14 specimens (Fig. 3F). At hatching, limbs are highly pigmented dorsally but almost unpigmented ventrally.

3.5. Tail (Figs. 1–3 and 5)

The tail bud appears at TS4 as a rounded, compact bump rising from the yolk mass. A small dextral vent tube appears partially fused to the tail bud and separates later at that stage (Fig. 3C). By TS5, the tail bud increases its size and appears indistinctly curved to either the right or the left side of the embryo. Fins are first very incipient but at late TS5 they begin to extend in a dorsoventral pattern. As development progresses, the vent tube locates more ventrally. The axial core of the tail lengthens at TS6 and the well-vascularized fins grow conferring an oblong shape to the tip of the tail. Histological sections through the tail at TS6 show the axial core with the dorsal fin, neural tube, notochord, muscles, and ventral fin all aligned in a dorsoventral pattern (Fig. 5). The core axis, together with the fins, are composed of a thin, single-layered, epidermis and connective tissue. A large blood vessel appears ventral to the notochord. By TS9 fins are very deep, giving the tail an almost circular aspect. Vascularization increases with numerous vessels immersed within the connective tissue (Fig. 5). The tail reaches full size at TS14, and is thicker but more maneuverable than in previous stages. The single hatched specimen available still exhibits vestiges of the tail fins (Fig. 2).

3.6. Endolymphatic calcium deposits (Fig. 1)

The endolymphatic calcium deposits (ECDs) are first visible at TS8 as a pair of small white spots situated posterior to the eyes. During TS9, the ECDs extend posteriorly into two creamy triangular structures. By TS12 (ca. 16 d.p.f.), they extend towards the midline of the vertebral region and, laterally, to the midpoint of the eyes. By TS13 they acquire their maximum size by the cephalo-caudal widening of the area and appear as two inverted triangles. By early TS14 they are masked by body pigmentation and at the end of the stage they are no longer visible.

3.7. Body integument (Figs. 1–3 and 6)

Embryos between TS4 and TS8 lack pigmentation and show a uniformly whitish color. By TS5, ciliated cells are scattered on the whole surface of the embryo body and yolk; ciliation is sparse on the dorsal aspect of the head (Fig. 3A and B). At TS6, dorsal, lateroventral and ventral integument have the same histomorphological organization which consists of a single-layer epidermis of cuboidal cells with large and lobulated nuclei; the dermis is barely identifiable and it seems to consist of loose collagen (Fig. 6A–C). Pigmentation is evident from TS8, with melanophores scattered on the dorsal aspect of the head and trunk. The proximal parts of limbs show melanophores from TS11. Pigmentation intensifies around TS13, when melanophores invade the ventral region. At TS14, the embryos are still almost fully ciliated, excepting the limbs, rostral, and dorsal regions of the head, and above the eyes (Fig. 3D and E). The dorsal, lateroventral, and ventral regions show histomorphological differences suggesting a dorsoventral pattern of integument maturation. In dorsal and lateroventral skin the basal cells of the epidermis begin to proliferate and become organized into layers of flattened cells; some developing mucous and serous glands are evident plus some scattered melanocytes. Below the epidermal basement membrane, a thin dermis of dense collagen fibers belonging to the stratum compactum is differentiated (Fig. 6D and E). The ventral integument shows a typically larval organization, consisting of a bilayered epidermis of cuboidal cells and a compact dermis. However, developing glands and scattered melanophores are already present (Fig. 6F).

3.8. Thyroid glands (Fig. 6)

By TS6 thyroid glands are already present and well differentiated. Thyroid glands are disposed ventral and lateral to the hyobranchial skeleton. Follicles are distinct and contain a central lumen and an epithelium formed of cuboidal cells; no accumulation of colloid is observed (Fig. 6G). At TS13, glands arrange as a pair of masses of well-developed follicles, ventral and lateral to the hyobranchial plate. Most lumina of thyroid follicles, which remain of a cuboidal epithelium, begin to accumulate colloid, and by TS14 most of them are fully filled (Fig. 6H).

4. Discussion

Due to the difficulty in finding fresh spawn in natural environments, few embryonic developmental studies were carried out in anurans with direct development. Our observations add new data to the limited information that exists so far on the ontogeny of these species.

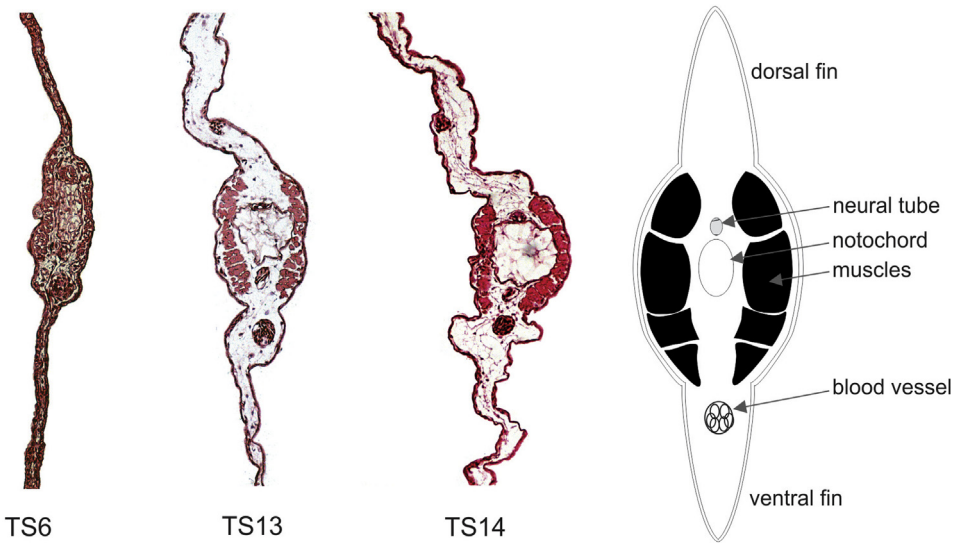

Fig. 5. Cross-sections of the tail in *Ischnocnema henselii* specimens at different stages. The neural tube/notochord axis is parallel to the sagittal plane of the body embryo, and caudal fins are dorsoventrally aligned.

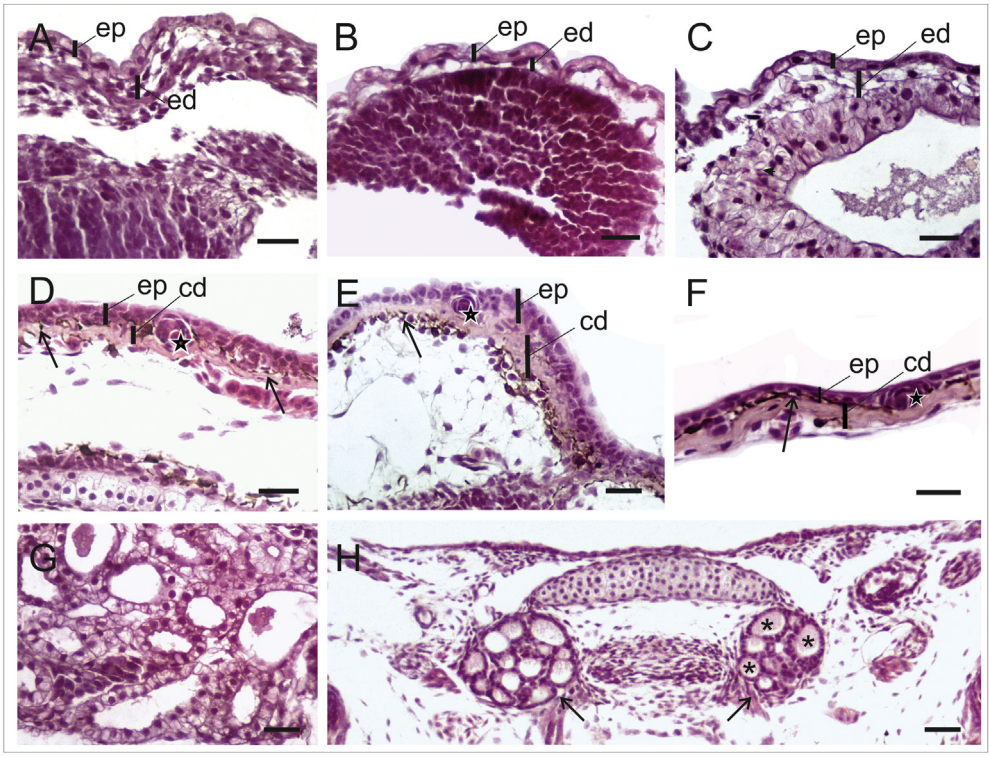

Fig. 6. Serial sections of the integument and thyroid glands of *Ischnocnema henselii* specimens at different stages. (A–F) Integument. Specimen at TS6, dorsal (A), lateroventral (B), and ventral (C) areas. Note the single layered epidermis of cuboidal cells. Specimen at TS14, dorsal (D), lateroventral (E), and ventral (F) areas. Note the lateroventral integument with a multilayered epidermis, developing glands (stars) and melanocytes (black arrows), and the ventral integument with bilayered epidermis and a continuous layer of melanocytes. (G, H) Thyroid gland histology. Specimen at TS6 (G), showing transverse section through follicles. Note the gland lumen without colloid. Specimen at TS14 (H), showing cross section of the thyroid gland (black arrows) and its relation with the hyoid plate. Note the colloid accumulation, with some follicles fully filled (asterisks). Abbreviations: cd = stratum compactum; ed = stratum spongiosum; ep = epidermis. Scale bars = 10 μm.

The developmental period that we estimated for *I. henselii*, between 28 and 30 days, is similar to that of the other two *Ischnocnema* species with available data (Lynn & Lutz 1946, 1947). This period is half the known developmental time to hatching of the confamilial *Brachycephalus ephippium* (Spix, 1824) (Pombal, 1999) and stands within the range of duration in other brachycephaloid species (Fig. 7). Comparisons within and outside of the terraranan clade reveal heterochronic shifts in the rate of species-specific stage progression. Regarding size, *I. henselii* hatchlings are comparable to most brachycephaloid species, that with the exception of large *Haddadus binotatus* (Spix, 1824) (about 9 mm; Goldberg & Vera Candioti, 2015) and small *B. ephippium* (5.5 mm; Pombal, 1999)

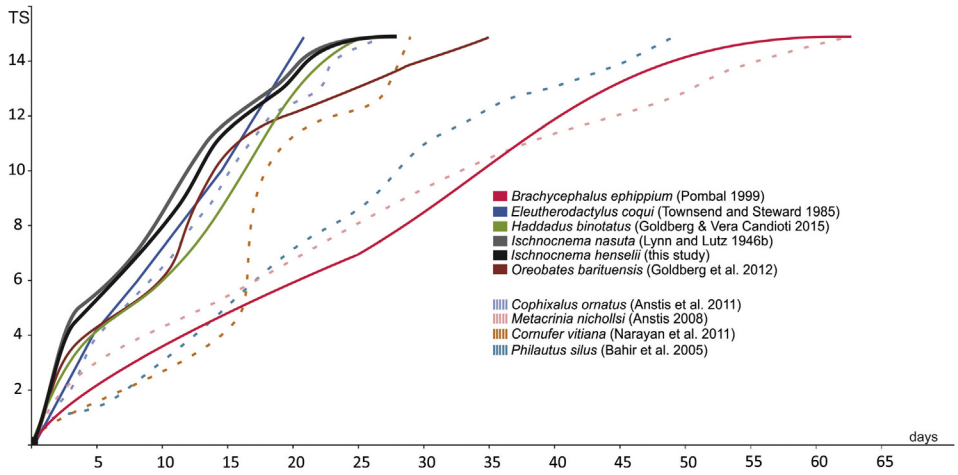

Fig. 7. Comparison of the rate of embryonic development in different anuran species with direct development. Continuous lines correspond to brachycephaloid species and dashed lines represent non-closely related taxa. Note the wide heterochronic variation in rate and offset of stage progression among species (Anstis 2008; Anstis et al. 2011; Bahir et al. 2005; Narayan et al. 2011).

are about 6 mm (e.g., Townsend & Stewart 1985; Lynn & Lutz 1946, 1947; Goldberg et al. 2012). Nevertheless, *I. henselii* froglets are small relative to their adult size (about 21.0–27.5 mm for males and 28.4–38.4 mm for females; Kwet & Solé 2005), which implies a significant posthatching growth.

As a staging table, that of Townsend and Stewart (1985) facilitates the identification of stages based on clearly defined external characters: neural grooves, limbs, eyes morphology, ECD, egg tooth, and pigmentation. Some of them exhibited variation in *I. henselii* regarding other known species, and are discussed as follows.

Variations in limb and gill development in direct developers have been deeply covered in previous contributions (e.g., Townsend & Stewart 1985; Goldberg et al. 2012; Schweiger et al. 2017). Instead of a synchronic onset of limb development, *I. henselii* embryos share an apparently precocious differentiation of hind limbs with the congeneric species (Lynn & Lutz 1946, 1947), *Eleutherodactylus portoricensis* Schmidt, 1927 (Gitlin, 1944), and with *H. binotatus* (Goldberg & Vera Candioti, 2015). Gills are also widely variable, even at an intrageneric level, including gills absent or barely discernible (e.g., as in Jameson 1950; Lynn 1942; Lynn & Lutz 1946, 1947; Goldberg et al. 2012; Goldberg & Vera Candioti 2015), well-defined projections (as in *I. henselii* and *E. portoricensis*; Gitlin 1944), and considerably developed gills in *E. coqui* (Townsend & Stewart 1985). In turn, an open ventral tube was previously described only in *Oreobates barituensis* Vaira and Ferrari 2008 (Goldberg et al. 2012).

A keratinized egg tooth is described in all known terrarananas and it is considered a synapomorphy of the clade (e.g., Hedges et al. 2008). Hardy (1984) studied the egg tooth in 36 species and described two different morphologies: a single, median, sharply-pointed to blunt-rounded structure, or alternatively a distinctly bifurcated structure. Embryos of *I. henselii* share the first type with several species of *Eleutherodactylus*, *Pristimantis*, and *Craugastor*, whereas the bifurcated configuration is reported in other *Eleutherodactylus* forms, *Oreobates*, and *Haddadus* (Hardy 1984; Goldberg et al. 2012; Goldberg & Vera Candioti 2015). This reinforces the idea of the high morphological variability in this group. An analogous keratinized structure called a caruncle develops as an epidermal thickening of the tip of the snout of *Sphenodon*, turtle, crocodile, and bird embryos (Clark 1961). While the distribution and origin of this structure (e.g., how it is different from the extraoral egg true teeth of squamates) has been widely discussed (e.g., Berkovitz & Shellis 2016), the nature of the brachycephaloid egg tooth and its relation with other oral keratinized anuran structures is still intriguing. Given the still open debate about the phylogenetic relationships of egg-brooding hemiphractids and Brachycephaloidea (see Castroviejo-Fisher et al. 2015), the presence of "keratinized tubercles" in embryos of the paraviviparous *Stefania* Rivero, 1968 is suggestive (Duellman & Hoogmoed 1984; Wassersug & Duellman 1984; Thibaudeau & Altig 1999).

The tail in brachycephaloid species is highly variable in size and shape. The observations of Nokhbatolfoghahai et al. (2010) focused attention on an additional aspect of variation: the arrangement of fins with respect to the axis formed by the aligned neural tube and notochord. Like *Eleutherodactylus* species, *B. ephippium*, and *Ischnocnema nasuta* (Lutz 1925) (e.g., Lynn & Lutz 1947; Townsend & Stewart 1985; Pombal 1999; author's unpubl. data), embryos of *I. henselii* exhibit a tadpole-like tail, with high fins arranged in a dorsoventral pattern throughout their ontogeny. Conversely, in fully developed tails of examined species of *Craugastor*, *Haddadus*, *Oreobates*, and *Pristimantis* fins dispose perpendicular to the core axis and have an extensive development, in some cases surrounding the embryo completely (a revision in Goldberg & Vera Candioti 2015). Fig. 8 shows a preliminary ancestral state reconstruction for the two characters, fin arrangement and extension, for known embryos of Brachycephaloidea. A tadpole-like tail with dorsoventral fins appears to be the plesiomorphic condition for this large clade, and lateral and expanded fins could be a putative synapomorphy for Craugastoridae. Much wider sampling and a robust analysis would be required to confirm this interpretation. The polymorphic tail extension of *O. barituensis* embryos (author's unpubl. data) raises new queries related to phenotypic plasticity during prehatching ontogeny of direct-developing species.

We are not aware of any detailed study describing changes that skin of direct-developing species undergoes throughout ontogeny. Adamson et al. (1960) provided a brief description in *Eleutherodactylus martinicensis* (von Tschudi 1838) at a stage likely corresponding to TS9, only mentioning a multicellular layer composed of cubical cells, with outer layer covered by a continuous cuticular deposit. As such, transformations in this species occur earlier than in *I. henselii*, probably in relation with its faster development (about 11 days). In metamorphosing anurans, maturation of the integument consists of transformations from larval to adult skin, which involve changes associated with the habitat transition from aquatic tadpoles to terrestrial adults. These transformations are generalized and described as a dorsal to ventral sequence of changes involving

Fig. 8. Preliminary ancestral state reconstruction of tail morphology in Brachycephaloidea. Tree topography is summarized after Padial et al. (2014), and tail morphology is taken from literature and authors personal observations (see text); state reconstruction was performed with software TNT (v. 1.5; Goloboff & Catalano 2016). The symmetric/asymmetric patterns of lateral fins differ in how perpendicular fins are regarding the muscular core axis (see Goldberg & Vera Candioti 2015). Note the association between fin arrangement and extension during brachycephaloid evolution.

an incremental number of epidermal layers, development of glands, and differentiation of two dermal strata (Duellman & Trueb 1986; Yoshizato 1992; Tamakoshi et al. 1998; Brown & Cai 2007). Intraspecific and interspecific comparison of spatiotemporal changes during the metamorphosis of larval integument suggests that it could vary between species (Tamakoshi et al. 1998; Fabrezi et al. 2010; Quinzio & Fabrezi 2012; Goldberg et al. 2019). However, in *I. henselii* the maturation of the integument has a typical dorsal to ventral sequence of changes as observed in most anurans of biphasic life cycle. As with the tail, this could be a plesiomorphic pattern that evolved only in derived groups, but this needs to be much more deeply explored.

Finally, the differentiation of thyroid glands occurs earlier in *I. henselii* regarding the available data for other direct-developing species (Lynn & Lutz 1947; Jennings & Hanken 1998). Although we register thyroid colloid accumulation at later stages than reported in other species (Lynn 1942; Lynn & Peadon 1955; Jennings & Hanken 1998), the gland's columnar epithelium indicates the peak of glandular activity (Etkin 1936; Grim et al. 2009). The embryonic onset of thyroid development in direct-developing amphibians differs markedly from the timing of thyroid development in metamorphosing taxa in which it occurs during the larval period, well after hatching (Etkin 1936). In amniotes, high levels of thyroid hormone occur at birth or hatching and are suggested to be related to the maturation of different organs and their relationship with the autonomy level of recently born/hatched specimens (Holzer & Laudet 2013; Buchholz 2015). The timing of thyroid development in *I. henselii* appears to be consistent with the hypothesis that the evolution of direct development in anurans involved a precocious activation of the thyroid axis (Jennings & Hanken 1998; Callery & Elinson 2000). In this sense, experimental approaches in *E. coqui* showed that thyroid axis inhibition affected the skin, limbs, jaw musculoskeleton, tail, and axial musculature (Callery & Elinson 2000).

As many previous studies, our results highlight the wide morphological and heterochronic diversity associated with the evolution of direct development, and the necessity of developmental tables that emphasize the specific characteristics of each taxon. New data will certainly reveal structural and temporal variations, including the evolution of novel traits that have arisen among direct-developing lineages of anurans.

Declaration of Competing Interest

None.

Acknowledgements

The work was funded by Agencia Nacional de Promoción Científica y Tecnológica (Argentina): PICT 510, PICT 2718, Consejo Nacional de Investigaciones Científicas y Técnicas: PIP 497; and São Paulo Research Foundation (FAPESP) grant #2013/50741-7. Fieldwork was partially funded by Plano de Ação Nacional para a Conservação dos Anfíbios e Répteis Ameaçados da Região Sul do Brasil (RAN/ICMBio). PPGT thanks FAPESP for the PhD fellowship grant #2014/05772-4 (2015–2018) and the Postdoctoral fellowship #2019/04076-8 (currently). We thank Instituto Chico Mendes de Conservação da Biodiversidade (ICMBio) for collection permits (#42108). T. H. Condez, J. P. C. Monteiro, D. Baeta, A. F. Sabbag, E. J. Comitti, P. C. A. Garcia, and I. Borel gave field assistance. CFBH was supported by São Paulo Reasearch Foundation (FAPESP), FAPESP/Fundação Grupo Boticário de Proteção à Natureza (grants #2013/50741-7 and #2014/50342-8, respectively), and Conselho Nacional de Desenvolvimento Científico e Tecnológico - CNPq (306623/2018-8). We thank Hendrik Müller and Mark Scherz for their helpful comments that improved the manuscript.

Appendix A. Supplementary data

Supplementary data to this article can be found online at https://doi.org/10.1016/j.jcz.2019.11.001.

References

Adamson, L., Harrison, R.G., Bayley, I., 1960. The development of the whistling frog, *Eleutherodactylus martinicensis* of Barbados. Proc. Zool. Soc. Lond 133, 453–469.
Anstis, M., 2008. Direct development in the Australian myobatrachid frog *Metacrinia nichollsi* from Western Australia. Rec. West. Aust. Mus. 24, 133–150.
Anstis, M., Purdy, J.D., Hawkes, T.R., Morris, I.B., Richards, S.J., 2011. Direct development in some Australopapuan microhylid frogs of the genera *Austrochaperina, Cophixalus* and *Oreophryne* (Anura: Microhylidae) from northern Australia and Papua New Guinea. Zootaxa 3052, 1–50.
Bahir, M.M., Meegaskumbura, M., Manamendra-Arachchi, K., Schneider, C.J., Pethiyagoda, R., 2005. Reproduction and terrestrial direct development in Sri Lankan shrub frogs (Ranidae: Rhacophorinae: *Philautus*). Raff. Bull. Zool. 12 (Suppl.), 339–350.
Berkovitz, B., Shellis, R.P., 2016. The Teeth of Non-mammalian Vertebrates. Academic Press, Cambridge.
Brown, D.D., Cai, L., 2007. Amphibian metamorphosis. Dev. Biol. 306, 20–33.
Brown, S.D.J., Collins, R.A., Boyer, S., Lefort, M.C., Malumbres-Olarte, J., Vink, C.J., Cruickshank, R.H., 2012. Spider: an R package for the analysis of species identity and evolution, with particular reference to DNA barcoding. Mol. Ecol. Res. 12, 562–565.
Buchholz, D.R., 2015. More similar than you think: frog metamorphosis as a model of human perinatal endocrinology. Dev. Biol. 408, 188–195.
Callery, E.M., Elinson, R.P., 2000. Thyroid hormone-dependent metamorphosis in a direct developing frog. PNAS 97, 2615–2620.
Castroviejo-Fisher, S., Padial, J.M., De la Riva, I., Pombal Jr., J.P., da Silva, H.R., Rojas-Runjaic, F.J.M., Medina-Méndez, E., Frost, D.R., 2015. Phylogenetic systematics of egg-brooding frogs (Anura: Hemiphractidae) and the evolution of direct development. Zootaxa 4004, 1–75.
Clark Jr., G.A., 1961. Occurrence and timing of egg teeth in birds. Wilson Bull. 73, 268–278.
Cope, E.D., 1862. On some new and little known American Anura. Proc. Acad. Nat. Sci. Philadelphia 14, 151–159.
Daudin, F.M., 1802. An. XI". Histoire naturelle des rainettes, des grenouilles et des crapauds, Quarto version. Levrault, Paris.
de Beer, G., 1940. Embryos and Ancestors. Oxford University Press, Oxford.
de Lima, A.V., Reis, A.H., Amado, N.G., Cassiano-Lima, D., Borges-Nojosa, D.M., Oriá, R.B., Abreu, J.G., 2016. Developmental aspects of the direct-developing frog *Adelophryne maranguapensis*. Genesis 54, 257–271.

Dietl, J., Engels, W., Solé, M., 2009. Diet and feeding behaviour of the leaf-litter frog *Ischnocnema henselii* (Anura: Brachycephalidae) in Araucaria rain forests on the Serra Geral of Rio Grande do Sul, Brazil. J. Nat. Hist 43, 1473–1483.
Duellman, W.E., Hoogmoed, M.S., 1984. The Taxonomy and Phylogenetic Relationships of the Hylid Frog Genus *Stefania*. Misc. Publ. Mus. Nat. Hist. Univ. Kansas 75, pp. 1–39.
Duellman, W.E., Trueb, L., 1986. Biology of Amphibians. Johns Hopkins University Press, London.
Duméril, A.M.C., Bibron, G., 1841. Erpétologie générale ou histoire naturelle complète des reptiles, vol. 8 (Librarie Enclyclopedique de Roret, Paris).
Etkin, W., 1936. The phenomena of the anuran metamorphosis. III. The development of the thyroid gland. J. Morphol. 59, 68–89.
Fabrezi, M., Quinzio, S.I., Goldberg, J., 2010. The ontogeny of *Pseudis platensis* (Anura, Hylidae): heterochrony and the effects of larval development on post-metamorphic life. J. Morphol. 271, 496–510.
Fabrezi, M., Quinzio, S.I., Cruz, J.C., Chuliver, M., Manzano, A., Abdala, V., Ponssa, M.L., Prieto, Y., Goldberg, J., 2017. Las interacciones entre el tiempo, la forma y el tamaño en la ontogenia animal. Cuad. Herpetol. 31, 103–126.
Fitzinger, L.J.F.J., 1826. Neue Classification der Reptilien nach ihren Natürlichen Verwandtschaften nebst einer Verwandtschafts-Tafel und einem Verzeichnisse der Reptilien-Sammlung des K. K. Zoologisch Museum's zu Wien, J. G. Heubner, Wien.
Foerster, N.E., Conte, C.E., 2018. Anuran diversity in an Araucaria Forest fragment and associated grassland area in a sub-tropical region in Brazil. Herpetol. Notes 11, 421–428.
Frost, D.R., 2019. Amphibian Species of the World: an Online Reference. American Museum of Natural History, New York, USA. Version 6.0 (12th July, 2019). Electronic Database accessible at. http://research.amnh.org/herpetology/amphibia/index.html.
Gitlin, D., 1944. The development of *Eleutherodactylus portoricensis*. Copeia 1944, 91–98.
Goldberg, J., Vera Candioti, F., 2015. A tale of a tail: variation during the early ontogeny of *Haddadus binotatus* (Brachycephaloidea: Craugastoridae) as compared with other direct developers. J. Herpetol. 49, 479–484.
Goldberg, J., Vera Candioti, F., Akmentins, M.S., 2012. Direct developing frogs: ontogeny of *Oreobates barituensis* (Anura: Terrarana) and the development of a novel trait. Amph. Rept 33, 239–250.
Goldberg, J., Quinzio, S.I., Cruz, J.C., Fabrezi, M., 2019. Intraspecific developmental variation in the life cycle of the Andean treefrog (*Boana riojana*): a temporal analysis. J. Morphol. 280, 480–493.
Goloboff, P.A., Catalano, S.A., 2016. TNT version 1.5, including a full implementation of phylogenetic morphometrics. Cladistics 32, 221–238.
Gosner, K.L., 1960. A simplified table for staging anuran embryos and larvae with notes on identification. Herpetologica 16, 183–190.
Grim, K.C., Wolfe, M., Braunbeck, T., Iguchi, T., Ohta, Y., Tooi, O., Touart, L., Wolf, D.C., Tietge, J., 2009. Thyroid histopathology assessments for the amphibian metamorphosis assay to detect thyroid-active substances. Toxicol. Pathol. 37, 415–424.
Günther, A.C.L.G., 1858. Neue Batrachier in der Sammlung des britischen Museums. Arch. Naturgesch 24, 319–328.
Hardy Jr., J.D., 1984. Frogs, egg teeth, and evolution: preliminary comments on egg teeth in the genus *Eleutherodactylus*. Bull. Md. Herpetol Soc. 20, 1–11.
Hedges, S.B., Duellman, W.E., Heinicke, M.P., 2008. New World direct-developing frogs (Anura: Terrarana): molecular phylogeny, classification, biogeography, and conservation. Zootaxa 1737, 1–182.
Heinicke, M.P., Duellman, W.E., Trueb, L., Means, D.B., MacCulloch, R.D., Hedges, S.B., 2009. A new frog family (Anura: Terrarana) from South America and an expanded direct developing clade revealed by molecular phylogeny. Zootaxa 2211, 1–35.
Holzer, G., Laudet, V., 2013. Thyroid hormones and postembryonic development in amniotes. Curr. Top. Dev. Biol. 103, 397–424.
Hoogmoed, M.S., Lescure, J., 1984. A new genus and two new species of minute leptodactylid frogs from northern South America, with comments upon *Phyzelaphryne* (Amphibia: Anura: Leptodactylidae). Zool. Mededelingen 58, 85–115.
Hughes, A., 1959. Studies in embryonic and larval development in Amphibia. I. The embryology of *Eleutherodactylus ricordii*, with special reference to the spinal cord. J. Embryol. Exp. Morphol. 7, 22–38.
IBGE, 2012. Manual Técnico da Vegetação Brasileira: Sistema Fitogeográfico, Inventário das Formações Florestais e Campestres, Técnicas e Manejo de Coleções Botânicas. Procedimentos para Mapeamentos, Rio de Janeiro.
Jameson, D.L., 1950. The development of *Eleutherodactylus latrans*. Copeia 1950, 44–46.
Jennings, D.H., Hanken, J., 1998. Mechanistic basis of life history evolution in anuran amphibians: thyroid gland development in the direct-developing frog, *Eleutherodactylus coqui*. Gen. Comp. Endocrinol. 111, 225–232.
Jiménez de la Espada, M., 1870. Fauna neotropicalis species quaedam nondum cognitae. J. Sci. Math. Phys. Nat 3, 57–65.
Jiménez de la Espada, M., 1872. Nuevos batrácios americanos. Anales Soc. Esp. hist. Nat 1, 84–88.
Katoh, K., Standley, D.M., 2013. MAFFT multiple sequence alignment software version 7: improvements in performance and usability. Mol. Biol. Evol. 30, 772–780.
Kwet, A., Solé, M., 2005. Validation of *Hylodes henselii* Peters, 1870, from southern Brazil and description of acoustic variation in *Eleutherodactylus guentheri* (Anura: Leptodactylidae). J. Herpetol. 39, 521–532.
Lucas, E.M., Molinari De Bastiani, V.I., Lingnau, R., 2018. Geographic distribution, habitat use and vocalizations of the leaf-litter frog *Ischnocnema henselii* (Anura: Brachycephalidae) in the subtropical Atlantic Forest. Rev. Bras. Zoociencias 19, 151–162.
Lutz, A., 1925. Batraciens du Brésil. C. R. Mém. Hebd. Séances Soc. Biol. Filial., Paris 93, pp. 211–214.
Lynn, W.G., 1942. The embryology of *Eleutherodactylus nubicola*, an anuran which has no tadpole stage. Contrib. Embryol 541, 27–62.
Lynn, W.G., Lutz, B., 1946. The development of *Eleutherodactylus guentheri* Stdnr. 1864. Bol. Mus. Nac. Zool 71, 1–46.
Lynn, W.G., Lutz, B., 1947. The development of *Eleutherodactylus nasutus* Lutz. Bol. Mus. Nac. Zool 79, 1–30.
Lynn, W.G., Peadon, A.E., 1955. The role of the thyroid gland in direct development in the anuran *Eleutherodactylus martinicensis*. Growth 19, 263–286.
Lyra, M.L., Haddad, C.F.B., de Azeredo-Espin, A.M.L., 2017. Meeting the challenge of DNA barcoding Neotropical amphibians: polymerase chain reaction optimization and new COI primers. Mol. Ecol. Resour 17, 966–980.
Madden, T., 2002. The BLAST sequence analysis tool. In: McEntyre, J., Ostell, J. (Eds.), The NCBI Handbook. National Center for Biotechnology Information (US), Bethesda (MD), pp. 281–296.
Martoja, R., Martoja-Pierson, M., 1970. Técnicas de Histología Animal, Toray-Masson S.A., Spain.
Narayan, E.J., Hero, M.J., Christi, K.S., Morley, C.G., 2011. Early developmental biology of *Platymantis vitiana* including supportive evidence of structural specialization unique to the Ceratobatrachidae. J. Zool. 284, 68–75.
Nieuwkoop, P.D., Faber, J., 1967. Normal Table of *Xenopus laevis* (Daudin). North-Holland Publishing Company, Amsterdam.
Noble, G.K., 1925. The Biology of the Amphibia. McGraw-Hill, New York.
Nokhbatolfoghahai, M., Mitchell, N.J., Downie, J.R., 2010. Surface ciliation and tail structure in direct-developing frog embryos: a comparison between *Myobatrachus gouldii* and *Pristimantis* (=*Eleutherodactylus*) *urichi*. Herpetol. J. 20, 59–68.
Padial, J.M., Grant, T., Frost, D.R., 2014. Molecular systematics of terraranas (Anura: Brachycephaloidea) with an assessment of the effects of alignment and optimality criteria. Zootaxa 3825, 1–132.
Palumbi, S.R., Martin, A.P., Kessing, B.D., McMillan, W.O., 1991. Detecting Population Structure Using Mitochondrial DNA. In: Hoelzel, A.R. (Ed.), Genetic Ecology of Whales and Dolphins. International Whaling Comission, Cambridge, pp. 203–215.
Paradis, E., Claude, J., Strimmer, K., 2004. APE: analyses of phylogenetics and evolution in R language. Bioinformatics 20, 289–290.
Peters, W.C.H., 1870. Über neue Amphibien (Hemidactylus, Urosaura, Tropdolepisma, Geophis, Uriechis, Scaphiophis, Hoplocephalus, Rana, Entomoglossus, Cystignathus, Hylodes, Arthroleptis, Phyllobates, Cophomantis) des Königlich Zoologisch Museum. Ber. Akad. Wiss. Berlin 1870, 641–652.
Pombal Jr., J.P., 1999. Oviposição e desenvolvimento de *Brachycephalus ephippium* (Spix) (Anura, Brachycephalidae). Rev. Bras. Zool. 16, 967–976.
Pyron, R.A., Wiens, J.J., 2011. A large-scale phylogeny of Amphibia with over 2,800 species, and a revised classification of extant frogs, salamanders, and caecilians. Mol. Phylogenetics Evol. 61, 543–583.
Quinzio, S., Fabrezi, M., 2012. Ontogenetic and structural variation of mineralizations and ossifications in the integument within ceratophryid frogs (Anura, Ceratophryidae). Anat. Rec. 295, 2089–2103.
R Core Team, 2017. R: a Language and Environment for Statistical Computing.
Reinhardt, J.T., Lütken, C.F., 1862. "1861". Bidrag til Kundskab om Brasiliens padder og Krybdyr. Förste afdeling: padderne og Öglerne. Vidensk. Medd. Dansk Naturhist. Foren. Ser 2 (3), 143–242.
Sampson, L., 1904. A contribution to the embryology of *Hylodes martinicensis*. Am. J. Anat. 3, 473–504.
Santos-Pereira, M., Almeida-Santos, M., Oliveira, F.B., Silva, A.L., Rocha, C.F.D., 2015. Living in a same microhabitat should means eating the same food? Diet and trophic niche of sympatric leaf-litter frogs *Ischnocnema henselii* and *Adenomera marmorata* in a forest of Southern Brazil. Braz. J. Biol. 75, 13–18.
Schmidt, K.P., 1927. A new tree-frog from Porto Rico. Am. Mus. Novit. 279, 1–3.
Schweiger, S., Naumann, B., Larson, J.G., Möckel, L., Müller, H., 2017. Direct development in African squeaker frogs (Anura: Arthroleptidae: *Arthroleptis*) reveals a mosaic of derived and plesiomorphic characters. Org. Divers. Evol. 17, 693–707.
Spix, J.B. von, 1824. Animalia nova sive Species novae Testudinum et Ranarum quas in itinere per Brasiliam annis MDCCCXVII–MDCCCXX jussu et auspiciis Maximiliani Josephi I. Bavariae Regis (München: F. S. Hübschmann).
Taboada, C., Grant, T., Lynch, J.D., Faivovich, J., 2013. New morphological synapomorphies for the New World direct-developing frogs (Amphibia: Anura: Terrarana). Herpetologica 69, 342–357.
Tamakoshi, T., Oofusa, K., Yoshizato, K., 1998. Visualization of the initiation and sequential expansion of the metamorphic conversion of anuran larval skin into the precursor of adult type. Dev. Growth Differ. 40, 105–112.
Taucce, P.P.G., Canedo, C., Parreiras, J.S., Drummond, L.O., Nogueira-Costa, P., Haddad, C.F.B., 2018a. Molecular phylogeny of *Ischnocnema* (Anura: Brachycephalidae) with the redefinition of its series and the description of two new species. Mol. Phylogenetics Evol. 128, 123–146.

Taucce, P.P.G., Canedo, C., Haddad, C.F.B., 2018b. Two new species of *Ischnocnema* (Anura: Brachycephalidae) from southeastern Brazil and their phylogenetic position within the *I. guentheri* series. Herpetol. Monogr. 32, 1–21.

Thibaudeau, G., Altig, R., 1999. Endotrophic anurans: development and evolution. In: McDiarmid, R.W., Altig, R. (Eds.), Tadpoles: the Biology of Anuran Larvae. University of Chicago Press, Chicago and London, pp. 170–188.

Thomas, R., 1966. New species of antillean *Eleutherodactylus*. Quart. J. Fla. Acad. Sci. 28, 375–391.

Townsend, D.S., Stewart, M.M., 1985. Direct development in *Eleutherodactylus coqui* (Anura: Leptodactylidae): a staging table. Copeia 1985, 423–436.

von Tschudi, J.J., 1838. Classification der Batrachier mit Berücksichtigung der fossilen Thiere dieser Abtheilung der Reptilien, Petitpierre, Neuchâtel.

Vaira, M., Akmentins, M.S., Attademo, M., Baldo, D., Barrasso, D., Barrionuevo, S., Basso, N., Blotto, B., Cairo, S., Cajade, R., Céspedez, J., Corbalán, V., Chilote, P., Duré, M., Falcione, C., Ferraro, D., Gutierrez, F.R., Ingaramo, M.R., Junges, C., Lajmanovich, R., Lescano, J.N., Marangoni, F., Martinazzo, L., Marti, R., Moreno, L., Natale, G., Pérez Iglesias, J.M., Peltzer, P., Quiroga, L., Rosset, S., Sanabria, E., Sanchez, L., Schaefer, E., Úbeda, C., Zaracho, V., 2012. Categorización del estado de conservación de los anfibios de la República Argentina. Cuad. Herpetol 26 (Suppl. 1), 131–159.

Vaira, M., Ferrari, L., 2008. A new species of *Oreobates* (Anura: Strabomantidae) from the Andes of northern Argentina. Zootaxa 1908, 41–50.

Valett, B.B., Jameson, D.L., 1961. The embryology of *Eleutherodactylus augusti latrans*. Copeia 1961, 103–109.

Wassersug, R.J., Duellman, W.E., 1984. Oral structures and their development in egg-brooding hylid frog embryos and larvae: evolutionary and ecological implications. J. Morphol. 182, 1–37.

Wiegmann, A.F.A., 1833. Herpetologischen Beyträge. I. Über die Mexicanischen Kröten nebst Bemerkungen über ihren verwandte Arten anderer Weltgegenden. Isis von Oken 26, 651–662.

Yoshizato, K., 1992. Death and transformation of larval cells during metamorphosis of Anura. Dev. Growth Differ 34, 607–612.